water

MDPI

Article

Effects of Operating Conditions on the Performance of Forward Osmosis with Ultrasound for Seawater Desalination

Bara A. K. Al-Sakaji [1], Sameer Al-Asheh [2] and Munjed A. Maraqa [1,3,*]

[1] Department of Civil and Environmental Engineering, College of Engineering, United Arab Emirates University, Al-Ain P.O. Box 15551, United Arab Emirates; sakajijust@yahoo.com
[2] Department of Chemical Engineering, College of Engineering, American University of Sharjah, Sharjah P.O. Box 2666, United Arab Emirates; sslasheh@aus.edu
[3] National Water and Energy Center, United Arab Emirates University, Al-Ain P.O. Box 15551, United Arab Emirates
* Correspondence: m.maraqa@uaeu.ac.ae

Abstract: This study investigates the effect of using ultrasound on water flux through a forward osmosis membrane when applied for seawater desalination. A synthetically prepared solution simulating seawater with scaling substances and organic foulants was used. The parameters considered include membrane cross-flow velocity, flow configuration (co-current versus counter-current), direction of ultrasound waves relative to the membrane side (active layer versus support layer), and type of draw solution (NaCl versus $MgCl_2$). The study revealed that applying a continuous ultrasound frequency of 40 kHz was effective in enhancing water flux, especially when the ultrasound source faces the membrane active layer, irrespective of the used draw solution. The highest water flux enhancement (70.8% with NaCl draw solution and 61.9% with $MgCl_2$ draw solution) occurred at low cross-flow velocity and with the ultrasound waves facing the membrane active layer. It was also observed that the use of ultrasound generally caused an adverse effect on the water flux when the ultrasound source faces the membrane support layer. Moreover, applying the ultrasound at the membrane support layer increased the reverse solute flux. For all tested cases, higher water flux enhancement was observed with NaCl as a draw solution compared to the cases when $MgCl_2$ was used as a draw solution.

Keywords: forward osmosis; ultrasound; water flux; concentration polarization; scaling; seawater

Citation: Al-Sakaji, B.A.K.; Al-Asheh, S.; Maraqa, M.A. Effects of Operating Conditions on the Performance of Forward Osmosis with Ultrasound for Seawater Desalination. *Water* **2022**, *14*, 2092. https://doi.org/10.3390/w14132092

Academic Editor: Thomas M. Missimer

Received: 3 June 2022
Accepted: 19 June 2022
Published: 30 June 2022

1. Introduction

The main processes in water desalination, that are mostly used worldwide, are phase change thermal-driven processes, such as multiple-effect distillation, multi-stage flash, and vapor compression; and single-phase mass transfer driven membrane-based processes, such as reverse osmosis (RO), ultrafiltration, and electrodialysis [1]. Since 2010 until the end of 2019, desalinated water capacity increased globally at an average yearly growth rate of around 7%. Up to mid-February 2020, the global cumulative desalinated water production capacity reached around 114.9 million m^3/d produced by around 21,000 plants [2]. Since 2010, the membrane-based desalination techniques were the most used methods in the desalination industry, where 90% of the awarded desalination contracts were based on membrane treatment systems, mainly RO systems [3]. However, most of the Middle East countries are still using thermal processes for large-scale capacity projects [3]. Thermal treatment processes are associated with high energy consumption and require costly infrastructures which are typically built adjacent to a power plant to supply the required heat source for steam generation [1].

Despite the several advantages associated with the RO systems, the relatively high-power demand needed by the process compared to the other treatment techniques that are used to treat low salinity feedwater and the high tendency for membrane fouling are still challenging concerns [4]. As such, there is a need to develop an efficient desalination

process in conjunction with other treatment processes such as precipitation [5], membrane distillation [6], ultrafiltration [7], nanofiltration [8,9] and RO [10,11]. It is expected that these processes would treat high salinity water, such as seawater and brine, and produce high-quality water in an economic manner by minimizing the energy requirements and reducing the fouling tendency. The forward osmosis (FO) membrane process is one of the feasible solutions for such challenges that has been recently considered [12]. Fortunately, its operating principle does not require an external high hydraulic pressure for process operation [13].

The FO technology is still under development. Many research ideas and scenarios were proposed toward further development and shifting the process from bench-scale or pilot plant to a reliable seawater commercialized scale application [14,15]. A few manufacturers, such as Modern Water plc, have installed and commissioned the world's first commercial FO seawater desalination plants for treating saline water (total dissolved solids of 55,000 mg/L) in Oman [16,17]. The limited implementation of the FO is due to some of the operational problems that make the process restricted to be properly used in large-scale commercial applications. Some of these limitations are related to the regeneration/separation of the draw solution, reverse solute diffusion from the draw solution side to the feed solution or vice versa, internal/external concentration polarization (ICP/ECP), and fouling problems [18,19]. These limitations have negative impacts on the system performance in terms of reduction in water flux and recovery rate, which ultimately affects the cost of water purification. While the FO process is expected to generally have a low surface fouling tendency compared to the RO [20], membrane fouling/concentration polarization cannot be ignored in the FO process and needs to be mitigated to enhance process performance and to have a better water flux [21]. In fact, various techniques for seawater desalination have been reported to mitigate FO membrane fouling/concentration polarization and thus enhance the process performance. These processes include conventional and non-conventional pretreatment systems, the use of chemical dosing, membrane surface modifications, optimization of system operating conditions, and selection of proper draw solution [21].

The use of ultrasound has been recently proposed as a pretreatment system or cleaning technique in water and wastewater membrane treatment and desalination applications that would enhance the membrane systems' performance. However, the use of ultrasound needs to be carefully selected, as applying ultrasound at certain frequencies and arrangements could cause damage to the membrane [22]. As summarized in Table 1, the use of ultrasound for flux enhancement has been recently considered in the FO process. However, the number of conducted studies is very limited and diverse in terms of the intended applications and testing conditions. Nonetheless, there is a consensus that coupling ultrasound with FO would enhance the water flux through the membrane under certain conditions [23–27]. The previously reported enhancement of flux with the use of ultrasound-assisted FO for water desalination could be challenged by the fact that most of these studies were not conducted using feed solutions that closely resemble brackish or seawater. For example, no experiments have been conducted to assess the effect of ultrasound on FO performance with a feed solution that contains scaling substances and organic foulants that are typically found in natural brackish and saline water. Hence, research is needed to better understand the effect of using ultrasound for FO systems using feed solutions that consists of saline waters that contains scalant, foulant, and algal materials at different operating conditions and different draw solutions.

This work intends to investigate the effect of some of the operating parameters pertinent to the use of ultrasound in conjunction with the FO membrane process for seawater desalination. The effects of membrane cross-flow velocity, flow configuration, direction of ultrasound waves relative to the membrane faces (active layer and supporting layer), and types of the draw solutions (sodium chloride and magnesium chloride) are considered in this study. The main objectives of this study are to (1) experimentally investigate the enhancement of FO membrane water flux using ultrasonic waves for synthetic seawater

through alteration of some of the operating parameters and (2) compare the system performance in terms of water flux for two types of draw solutions, namely sodium chloride (NaCl) and magnesium chloride ($MgCl_2$). The study was designed to address the following questions: Will utilizing ultrasound with the FO system enhance the water flux when desalinating synthetic seawater containing scalant substances and organic foulants? What would be the effect of changing the cross-flow velocity (CFV) of the feed and the draw solution on the flux with and without the use of ultrasound irradiation? Will the flow configuration of the FO system have an impact on the water flux in the absence and presence of ultrasound irradiation? How does the flux change with the change in the ultrasound source location relative to the FO membrane layers? By addressing these questions, a better understanding of the impact of ultrasound-assisted FO for water desalination will be gained, which will contribute to the enhancement of the system performance.

Table 1. Previous studies of ultrasound-assisted FO [1].

Study Purpose	Membrane Type	Feed Solution	Draw Solution	US Frequency (kHz)	US Operation	CFV (cm/s)	Flow Mode	Reference
Mitigate internal concentration polarization	TFC	Tannin	Na_2SO_4	20, 573, 1136	Continuous/ Intermittent	-	-	[28]
Concentrate fruit juice and natural colorant	CTA	Sweet lime/Rose extract	NaCl	30	Intermittent	78.9	C	[23]
Sludge dewatering	CTA	Synthetic sludge	NaCl	40	Intermittent	-	-	[24]
Mitigate scale and colloidal fouling	CTA	NaCl with $CaSO_4$ or silica	NaCl	72	-	8	CC	[29]
Desalination	CTA	NaCl	NaCl	25, 45, 72	-	-	CC	[25]
Desalination	CTA	NaCl	$MgSO_4$, $CuSO_4$	40	Continuous	1.1	C	[26]
Desalination	CTA	DI	NaCl	-	Continuous	8.5	CC	[27]

[1] TFC: Thin film composite, CTA: Cellulose triacetate, CFV: Cross-flow velocity, DI: Deionized water, US: Ultrasound, C: Co-current, CC: Counter-current.

2. Materials and Methods

2.1. Material

The feed solution was prepared using different materials to simulate, as closely as possible, the seawater characteristics in terms of salinity, scaling substances, and algae. Sodium chloride (NaCl) was used to represent the dissolved solids content [26], calcium sulfate dihydrate ($CaSO_4 \cdot 2H_2O$) was used to represent inorganic fouling and scaling substances [29–31], and sodium alginate was used to simulate the biofouling algal organic matter that would exist in seawater intakes [32]. The initial concentration of the draw solution was fixed in all tests at 4.5 M (262.98 g/L) for NaCl and at 2 M (190.42 g/L) for $MgCl_2$. These concentrations resulted in almost equal osmotic pressure values of about 225 atm [33], which allows comparison between the flux behavior at similar osmotic pressure gradients of draw solutions having monovalent and divalent cations.

The simulated seawater feed solution was prepared by dissolving 40 g of NaCl (99.9% assay, Fisher chemical®, Amsterdam, The Netherlands), 5.059 g $CaSO_4 \cdot 2H_2O$ (99.9% assay, Fisher chemical®, Amsterdam, The Netherlands), and 300 mg of sodium alginate (CAS No. 9005-38-3, HIMEDIA®, Maharashtra, India) in 1 L DI water (conductivity <0.067 µS/cm) to obtain a final solution of 44,300 mg/L. Two draw solutions were prepared separately in this study, namely NaCl and $MgCl_2$. The NaCl solution was prepared by dissolving the proper amount of NaCl in DI water to obtain a final concentration of 4.5 M (262.98 g/L) NaCl, whereas the $MgCl_2$ was prepared by dissolving the required amount of $MgCl_2 \cdot 6H_2O$ (≥0.99% assay, Rankem®, Ghaziabad, India) in DI water to obtain a final concentration of 2 M (190.42 g/L) $MgCl_2$. Each prepared solution was mixed for around 20 min. The used DI water was produced by a water desalination unit (ELGA, LA737, Veolia, High Wycombe, UK).

FTSH2O™ flat sheet cellulose triacetate (CTA)-embedded support FO membranes were used in this study. The membranes were manufactured by Fluid Technology Solution, Inc. (Albany, NY, USA) and procured from Sterlitech (Auburn, WA, USA).

2.2. Experimental Work

In this study, three operational parameters were selected to investigate the effect of using ultrasound on FO membrane process performance (water flux) for seawater desalination. These include CFV at both membrane sides, flow configuration arrangement, and membrane orientation toward the ultrasound source. These parameters were tested for two types of draw solutions (NaCl and $MgCl_2$). Fixed feed and draw solutions CFV at two velocity levels were selected. Two flow configuration arrangements, co-current (the feed and draw solutions flow in the same direction) and counter-current (the feed solution flows in the opposite direction of the draw solution flow) were considered. The exposure of the membrane surface to ultrasound was also tested either with the active layer facing the transducer or with the support layer facing the transducer. Eight cases were tested with the use of ultrasound for each draw solution; duplicate runs were conducted for each case. A summary of the investigated cases of the deployed ultrasound irradiation is given in Table 2. For each draw solution, the cases are named by the applied CFV, followed by the current configuration, followed by the used ultrasound arrangement. For each case, a baseline experiment (with duplicate runs) was conducted at the full-intended experimental conditions without having the ultrasound bath on board. The baseline cases for each draw solution are named by the applied CFV, followed by the flow configuration, followed by BL to denote baseline conditions. In all the investigated cases, the feed solution was introduced, tangentially, to the membrane active layer (smooth surface) while the draw solution was at the side of the membrane support layer (rough surface). The tested cases were randomized to minimize the effect of external factors on the results.

Table 2. Testing arrangement for NaCl and $MgCl_2$ draw solutions with the use of ultrasound.

Case [1]	Run	Draw Solution Test Order		CFV (cm/s)	Flow Configuration	Transducer Location
		NaCl	$MgCl_2$			
0.25-C-AL	1st	10	10	0.25	Co-current	Active layer
	2nd	11	11	0.25	Co-current	Active layer
1.0-C-AL	1st	8	2	1.0	Co-current	Active layer
	2nd	12	14	1.0	Co-current	Active layer
0.25-CC-AL	1st	13	5	0.25	Counter-current	Active layer
	2nd	16	12	0.25	Counter-current	Active layer
1.0-CC-AL	1st	14	8	1.0	Counter-current	Active layer
	2nd	15	16	1.0	Counter-current	Active layer
0.25-C-SL	1st	2	3	0.25	Co-current	Support layer
	2nd	9	13	0.25	Co-current	Support layer
1.0-C-SL	1st	5	7	1.0	Co-current	Support layer
	2nd	7	9	1.0	Co-current	Support layer
0.25-CC-SL	1st	1	6	0.25	Counter-current	Support layer
	2nd	3	1	0.25	Counter-current	Support layer
1.0-CC-SL	1st	4	4	1.0	Counter-current	Support layer
	2nd	6	15	1.0	Counter-current	Support layer

[1] In naming the tested cases, the number refers to the CFV, C denotes co-current flow, CC denotes counter-current flow, AL denotes ultrasound facing the membrane active layer, and SL denotes ultrasound facing the membrane support layer.

2.3. Experimental Setup and Procedure

A fresh membrane was used for each test. Following the manufacturer's recommendations, the membrane sheet was cut to suit the testing cell dimensions and rinsed with deionized (DI) water to remove the membrane preservative solution. The membrane sheet was housed in a prefabricated, fully sealed, FO membrane testing cell. The cell consisted of two channels separated by the FO membrane. Each channel had an internal length of

81 mm, a width of 60 mm, and a depth of 24 mm, providing a membrane active area of around 48.6 cm^2. The cell housing design allows both system solutions (feed and draw solutions) to flow tangentially to the membrane sides (active and support layers) by having inlet and outlet ports fitted with the acrylic channels. The cell cover is fabricated from acrylic materials with 2 mm thickness to facilitate the functionality of the ultrasound waves. Rubber gaskets (3 mm EPDM) were provided between the two mating parts of the cell to ensure proper system sealing. Stainless steel studs, washers, and nuts were used to ensure proper assembly of cell parts. Stainless steel frames with 5 mm thickness were also used on the top of the acrylic sheet to avoid any deformation in the acrylic sheets The components of the membrane testing cell housing unit used in this work are presented elsewhere [26].

Depending on the required flow configuration (co-current or counter-current), an appropriate piping system was connected to the testing cell ports. The simulated seawater feed solution was delivered to the unit using a diaphragm pump (Model TYP-9600-KJ, Deng Yuan Industrial Co., Ltd., Taichung, Taiwan) in a closed-loop storage graduated cylinder (1 L capacity). The feed solution storage was placed on top of the digital balance to measure the change in its weight over time. The draw solution recirculation pumping was measured in the same way, where the draw solution was pumped tangentially to the membrane support layer at a CFV equal to the feed solution flow velocity and returned to the draw solution storage graduated cylinder (1 L capacity) by another pump similar to the one used for pumping the feed solution. The required CFV (flow rate/cell cross-sectional area) was obtained by changing the pump flow rate. To obtain a CFV of 0.25 and 1.0 cm/s, the pump flow rates were fixed at around 0.3 and 1.1 L/min, respectively. When the system was completely assembled, air bubbles inside the system were released by pumping the feed and draw solution for a short time. For all tests, the initial volumes of the feed and draw solutions were both kept the same at around 670 mL. This value was mainly selected to have a buffer volume in the draw solution cylinder so as to accommodate the water molecules transferred from the feed solution toward the draw solution cylinder.

The effect of ultrasound on the membrane flux was studied using a continuous ultrasonic wave at a fixed frequency of 40 kHz. In this case, the previously described testing cell was placed in the ultrasonic bath cleaner (Capacity: 5.7 L, Model No. 3510 DTH Ultrasonic Cleaner, Branson Ultrasonics, CT, USA) filled with potable water and located 20 mm from the bottom of the tank. The device was fitted with two built-in transducers fixed at the bottom of the tank. Based on the required membrane face orientation toward the transducer location, the testing cell was oriented. The experimental setup for one of the tested arrangements is illustrated in Figure 1.

For all the FO experiments, the feed and draw solutions temperatures were kept constant at around 24 $\pm$ 1 °C. To maintain the temperature of the ultrasound bath, the potable water was recirculated inside the tank. Changes in the weight of the feed solution, conductivity, temperature (Hanna instruments edge EC, HI2003, Edge dedicated EC, HI763100, Crișana, Romania), and pH (Model: MW801, Milwaukee instruments, Rocky Mount, NC, USA) were measured. The draw solution temperature, pH, and the ultrasound bath temperature were also monitored. The average pH of the feed and draw solutions for all the cases was about 6.6 with a deviation from the average of no more than 0.2 pH units during any of the tested runs. To avoid excessive dilution of the draw solution, the duration of each run lasted 140 min, with readings of the weight and the conductivity of the feed solution taken every 10 min, starting 20 min after the initiation of the run.

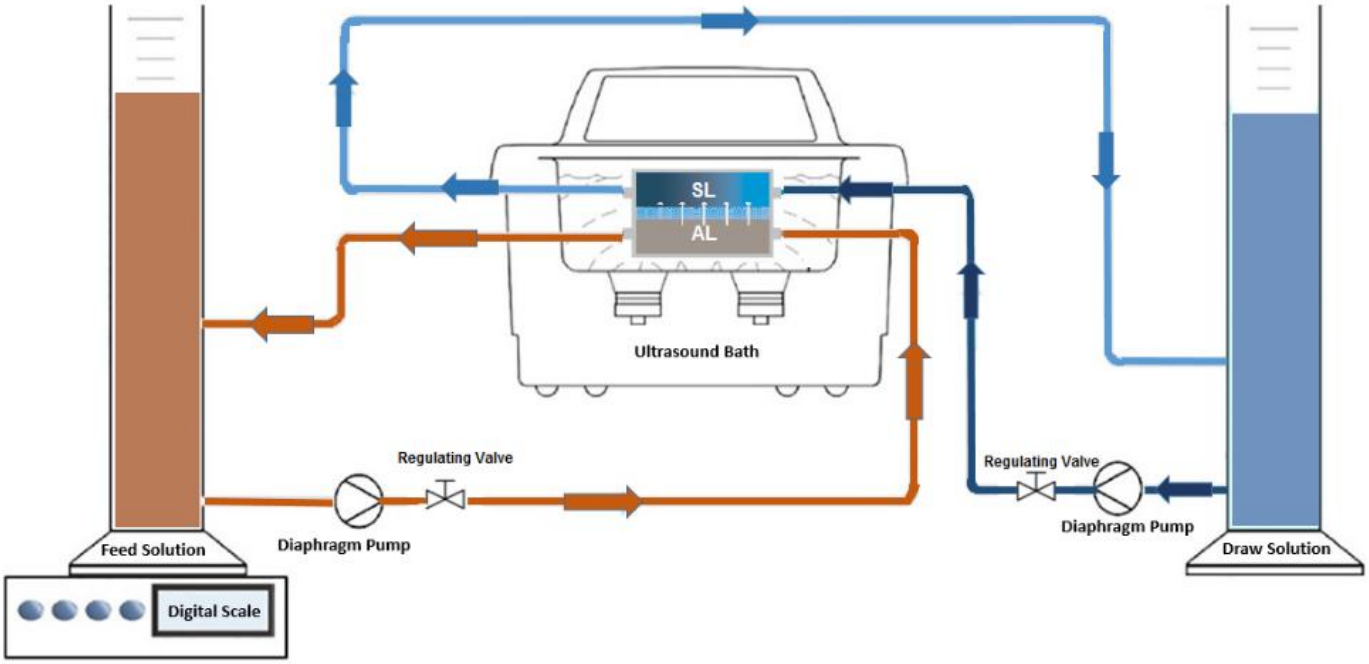

Figure 1. Experimental setup arrangement in ultrasound-assisted FO process with co-current flow and the active layer facing the ultrasound transducer.

2.4. Membrane Water Flux Calculation

In the FO system, the difference in the osmotic pressure between the draw and feed solutions is the driving force for water flux across the membrane. Generally, the effective osmotic pressure difference is lower than the bulk osmotic pressure difference owing to the effect of concentration polarization. This in turn reduces the actual water flux through the membrane [33,34]. The flux is also influenced by the resistivity of water to diffuse through the membrane, which is dependent on the membrane structural properties and the water diffusion coefficient. The former is affected by the thickness, tortuosity, and porosity of the membrane [35]. Aside from the FO membrane characteristics and the osmotic pressure difference, the flux through the membrane is influenced by the system operating conditions (flow velocity and flow configuration) [21,36]. Meanwhile, the presence of scaling substances and fouling materials in the feed solution adversely affects the water flux through the membrane due to internal or external clogging of the membrane layer [37].

In this study, the FO process performance was measured by the water flux produced by the membrane. Membrane water flux was calculated based on measuring the change in the mass of the feed solution throughout the respective experiment test according to the following equation [26]:

$$J_w = \frac{\Delta m}{\rho_w S \Delta t} \quad (1)$$

where J_w is the water flux (L/m^2·h), Δm is the change in the mass of the feed solution (g), ρ_w is the water density (assumed to be 1000 g/L), S is the membrane effective surface area (m^2), and Δt is the duration that corresponds to Δm (h).

3. Results and Discussion

Figure 2 shows examples of changes in water flux with time for some of the tested cases with NaCl and $MgCl_2$ draw solutions. For all tested cases, there was a general drop in water flux over time, which could be partially attributed to the lower driving force for water permeation across the membrane caused by a decrease in the osmotic pressure difference between the draw solution and the feed solution. The drop in the water flux over time was more pronounced for the cases with the higher CFV due to the higher flux

observed with these cases. However, the overall drop in the water flux was more severe for the cases with low CFV.

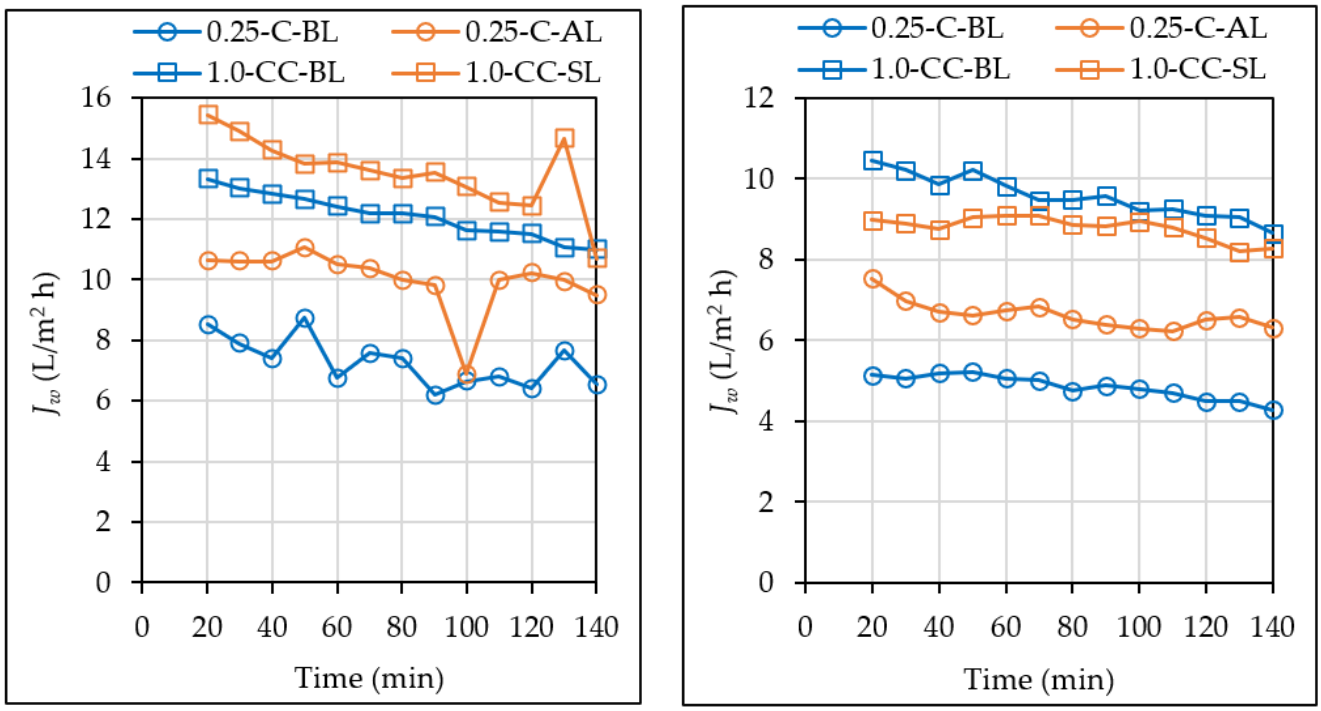

Figure 2. Changes in flux with time for runs of the tested cases with (**a**) NaCl and (**b**) $MgCl_2$ draw Scheme 0. C-BL and 1.0-CC-BL) and with the ultrasound facing the active layer (0.25-C-AL) or facing the support layer (1.0-CC-SL) of the membrane. In naming the baseline cases (i.e., without ultrasound), C denotes co-current flow, CC denotes counter-current flow, and BL denotes baseline conditions.

The values of the flux of the feed solution for all the tested cases are presented in the supplementary material. Analysis of the data revealed that the average water flux among the two runs of all the investigated cases deviates, on average, by 8.9% with a standard deviation of 7.1%. In the remainder of the analysis, the average water flux for each investigated case is presented, which was determined based on the water flux calculated every 10 min for the two runs of the case.

Section 3.1 presents the average water flux through the FO membrane with and without using ultrasound for the NaCl draw solution. Results of the average water flux when $MgCl_2$ was used as a draw solution are presented in Section 3.2. Comparison of the average water flux produced by NaCl and $MgCl_2$ draw solutions is presented in Section 3.3, while suggested future work is presented in Section 3.4.

3.1. Effect of NaCl as a Draw Solution

Considering the previously described cases of the experimental work as summarized in Table 2, baseline tests for NaCl as a draw solution were conducted to determine the membrane performance in the absence of the ultrasound source (i.e., no active or support layer effect). The average membrane water flux (J_w) against the respective cases with and without the use of ultrasound is shown in Figure 3.

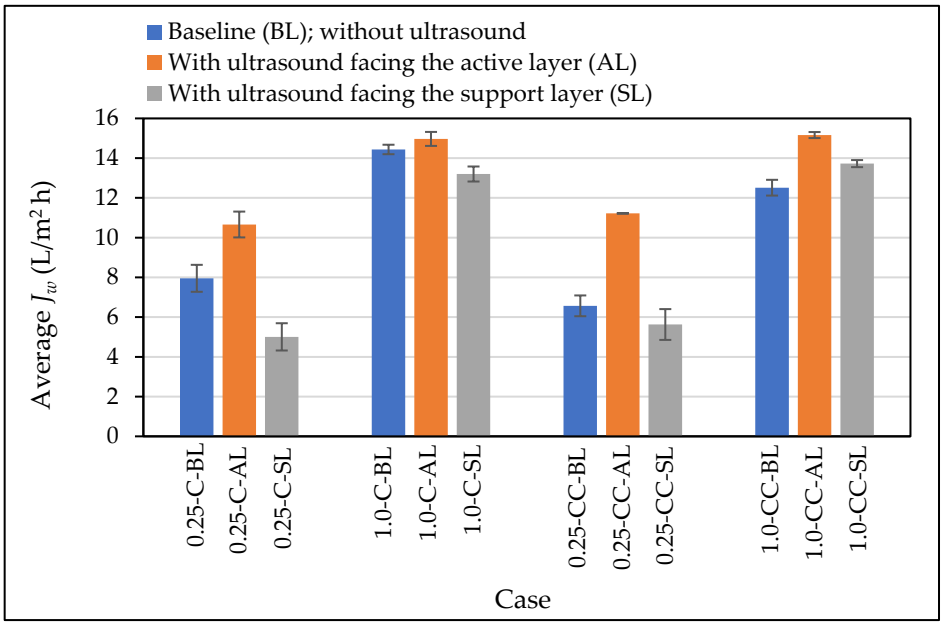

Figure 3. Average J_w for the cases with and without the use of ultrasound for NaCl draw solution. The error bar represents the lower and upper average J_w associated with the two runs of the tested case.

3.1.1. Baseline Conditions

Figure 3 indicates that the highest water flux without the use of ultrasound was obtained with the case 1.0-C-BL, where the average flux was 14.44 L/m^2·h, and the lowest flux value of 6.57 L/m^2·h was obtained with the case 0.25-CC-BL. For both flow configurations (co-current and counter-current), the membrane water flux increased with increasing the CFV (Figure 3). Increasing the CFV from 0.25 to 1.0 cm/s in the co-current and counter-current arrangements increased the water flux by about 81.5% and 90.5%, respectively. Regarding the system flow configurations, at a CFV of 0.25 cm/s, the average water flux decreased from 7.95 to 6.57 L/m^2·h, with the shift from the co-current to the counter-current configuration (Figure 3). At a CFV of 1.0 cm/s, the average water flux also decreased from 14.44 to 12.51 L/m^2·h, with the shift from the co-current to the counter-current configuration. The above values have been considered as a baseline to study the effect of the membrane flux performance with the use of ultrasound.

3.1.2. Effect of Ultrasound on Membrane Performance

The effect of ultrasound on the membrane average water flux was investigated at different testing arrangements, namely 0.25-C-AL, 1.0-C-AL, 0.25-CC-AL, 1.0-CC-AL, 0.25-C-SL, 1.0-C-SL, 0.25-CC-SL, and 1.0-CC-SL. The results are presented in Figure 3 along with those obtained under baseline conditions. Compared to the baseline results, the average water flux increased when the ultrasound source faced the membrane active layer. Moreover, the average water flux was lower except for the case of 1.0-CC- SL, when the ultrasound source faced the membrane support layer.

The most significant water flux improvement due to the use of ultrasound was observed for the case of 0.25-CC-AL (Figure 3), where the average flux increased from 6.57 L/m^2·h, under baseline conditions, to 11.22 L/m^2·h, when ultrasound was applied (i.e., 70.8% improvement). For the case of 0.25-C-AL, the average water flux increased from a baseline value of 7.95 L/m^2·h to 10.66 L/m^2·h by applying ultrasound (an improvement of 34.0%). Applying the ultrasound in the case of 1.0-CC-AL caused an improvement in the average water flux by 21.2% (the average water flux increased from 12.51 to 15.16 L/m^2·h). However, for the case of 1.0-C-AL, there was only a slight increase in the average water flux

(from 14.44 to 14.97 L/m^2·h), which is considered insignificant given the overlap between the range of the average water flux with and without the use of ultrasound for that case.

When the ultrasound source was in the direction of the membrane active layer, it was observed that the highest water flux improvement caused by the ultrasound was more significant for the cases with the low CFV. This could be mainly attributed to the formation of fouling and scaling layers, which are caused by the presence of sodium alginate and calcium sulfate in the feed solution, and the initiation of ECP that was promoted during the low CFV at the membrane active layer side. Imposing the ultrasound reduces the formation of these layers, which ultimately enhances the membrane water flux. Moreover, the effect of the ultrasound on the membrane water flux improvement at high velocity was less significant compared to that observed at low velocity. This could be due to the effect of the high CFV on the membrane surface cleaning and its role in minimizing the ECP. Examples of the SEM images for fouling membranes at low and high CFV are shown in Figure 4. The figure demonstrates the increase in membrane fouling with the ultrasound facing the support layer and at low CFV (Figure 4c,d) as opposed to when the ultrasound faces the active layer with high CFV (Figure 4e,f).

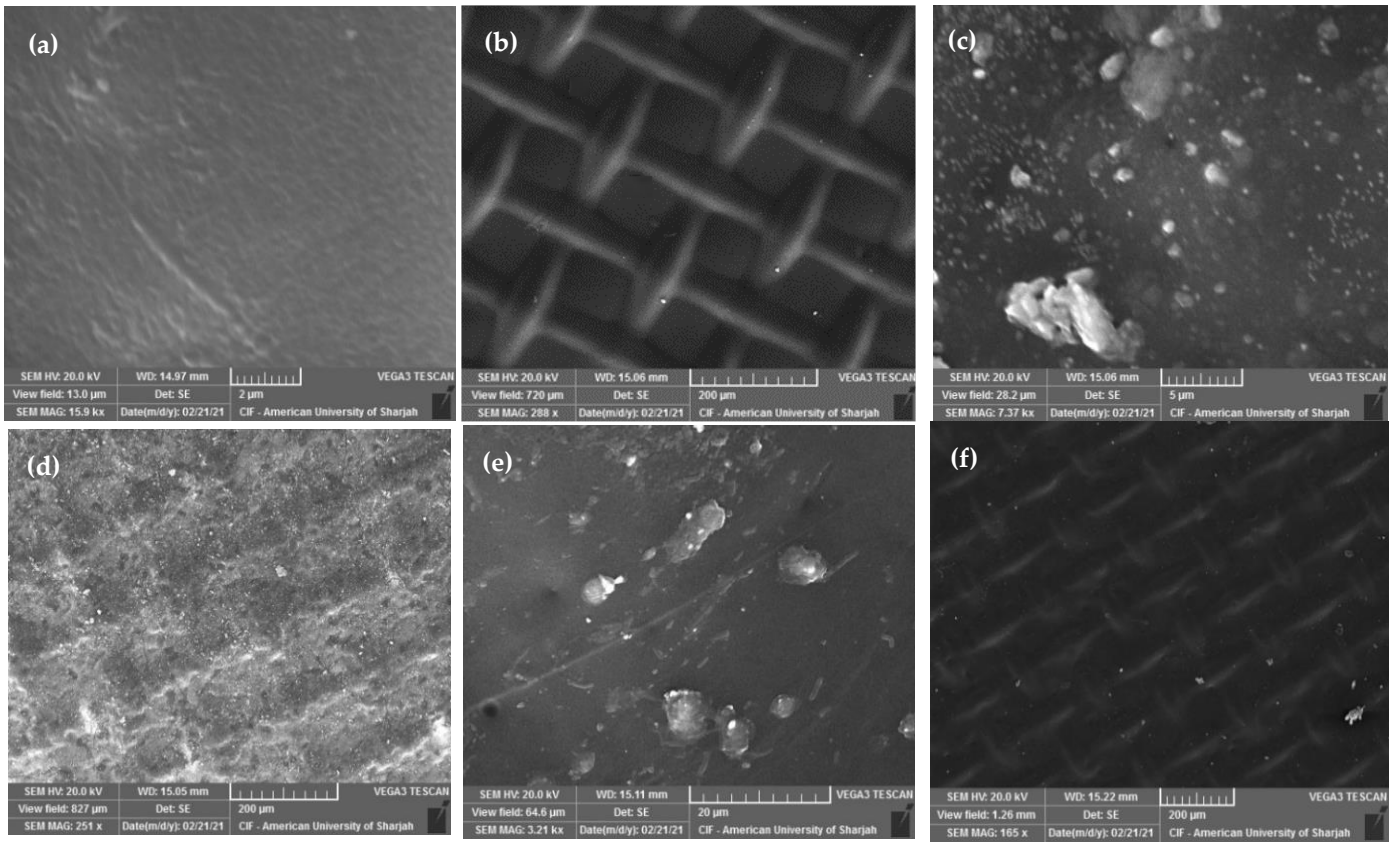

Figure 4. SEM images of the original membrane (**a**) active layer and (**b**) support layer, the membrane after use for the (**c**) active layer and (**d**) support layer at low CFV with the ultrasound facing the support layer (Case 0.25-CC-SL with NaCl draw solution), and the membrane after use for the (**e**) active layer and (**f**) support layer at high CFV with the ultrasound facing the support layer (Case 1.0-CC-AL with $MgCl_2$ draw solution).

Changes in the flow configuration at similar CFVs for the case with the ultrasound source facing the active layer caused a very low impact on flux enhancement. This could be attributed to the small dimensions of the testing cell, where the effect of changing the flow configuration does not appear to be clearly noticeable along the selected membrane dimensions. This agrees with the findings of Phuntsho et al. [38], who found no significant

effect on the water flux due to the change in the flow configuration, which was also attributed to the small size of the testing cell.

Considering the feed solution characteristics of having fouling and scaling materials, the active layer of the FO membrane is exposed to fouling problems that ultimately cause flux reduction due to cake/gel layer formation (external fouling). In this study, both sodium alginate and calcium sulfate are present in the feed solution. When alginate interacts with the solution containing calcium sulfate, a layer of calcium alginate is immediately formed to surround the sodium alginate surface. The negatively charged sulfate ions in the solution are attracted by the calcium ions, resulting in the formation of a new layer of SO_4^{2-} that promotes crystal formation and acts as a nucleus around the sodium alginate molecules, which forms a combined network of calcium sulfate crystals and an alginate gel layer [39]. This compacted gel layer promotes membrane surface fouling and reduces water flux [30,40,41]. Moreover, the high concentration of solutes in the feed solution adjacent to the membrane active layer, compared to the feed solution bulk concentration, results in the formation of an ECP boundary layer on the membrane active layer that reduces the osmotic pressure difference [42]. In addition, an accelerated cake-enhanced osmotic pressure (CEOP), due to reverse solute flux, causes the formation of a thick fouling layer on the membrane surface due to the unavailability of hydraulic pressure. The formation of the CEOP causes flux reduction by increasing the system resistance and decreasing the net osmotic pressure driving force due to the trapped solute particles between the membrane active layer and the formed fouling layer [43,44]. This is in agreement with Heikkinen et al., who observed flux enhancement upon applying ultrasound on the CTA membrane active layer [28].

It is reported that the use of ultrasound minimizes the impact of ECP by (1) reducing solute concentration at the membrane boundary layer, (2) reducing the external fouling effect by breaking the fouling (sulfate crystals and alginate gel) layer formed [29], and (3) detaching the deposited substances on the membrane active layer [45]. This significantly reduces the system resistance and increases the membrane performance accordingly. Ultrasound waves produce a high mechanical power through a physical medium (water) by a little mechanical movement [22]. The propagation of sound waves starts by a group of cyclic compression and rarefaction waves that may cause physical/chemical changes at different levels and magnitudes in the medium. Due to the compression and rarefaction cycles, the medium molecules are exposed to a positive and negative acoustic pressure that creates bubble cavitation [46]. Bubbles keep growing to a certain size and then collapse. Bubbling collapse produces extreme pressure, up to 1000 atm, and localized temperature up to 5000 K [26,47]. This phenomenon (local hotspots) enhances the heat transfer rates within the feed solution and promotes the creation of a highly turbulent area [26] that can be used to detach the deposited particles on the membrane surface and, thus, enhances the performance by increasing water flux. Moreover, the observed flux enhancement in the ultrasound source facing the active layer could be also attributed to the ultrasound effect of generating local heating zones on the membrane surface that could accelerate transfer rates.

The use of ultrasound could assist in membrane surface cleaning through mechanisms such as acoustic streaming, microstreaming, microstreamers, microjets, and shock waves [48]. The acoustic streaming mechanism enhances membrane cleaning by transmitting acoustic energy through the feed solution to produce liquid flow which is obstructed, causing unidirectional liquid flow waves with a flow velocity that reaches up to 10 m/s parallel to the surface of the deposits, which may help in foulant removal [26]. Microstreamers, on the other hand, are generated by the superimposition of the ultrasound waves produced by the transducer and the waves reflected from the membrane surface to create standing (stationary) waves. The cavitation bubbles are attracted by the standing wave antinodes and structured in a certain path where the bubble size increases while traveling toward the antinodes located at the membrane surface. Once the antinodes reach the fouled membrane surface, bubbles are formed, causing drag and a detach effect on the particles

deposited on the membrane surface [22,26,49]. Microstreaming may also play a role in membrane fouling cleaning by creating shear/drag forces used to detach the foulants from the membrane surface. During the compression and expansion cycles, a rapid fluctuation (in magnitude and direction) occurs in the fluid movement caused by oscillation in the cavitation bubbles. The shrinking effect of the cavitation bubbles pulls the liquid molecules away from the membrane surface, while the expanding effect pushes the molecules to the membrane surface, causing shear and drag forces needed for foulant removal from the membrane surface [50].

Microjets produced by the ultrasound is another mechanism that can clean the fouled membrane surface by creating the pitting and scrubbing effects on the fouling layer. Microjets create turbulent zones in the feed solution by their ability to attain high-velocity fluid jets (100–200 m/s) due to the asymmetric cavitation bubble collapse [22]. Shock waves produced by the ultrasound also show the capability to clean the membrane surface and provide high pressure toward the membrane active layer that ultimately contributes to water flux enhancement. Shock waves are generated continuously during the compression and expansion cycles. When the cavitation bubble reaches its minimum size, at the end of the compression cycle, the cavitation bubbles reach a sudden halt causing liquid molecules, moved to the bubbles, to reflect with high pressure toward the membrane surface [26,50].

It should be indicated that in the FO membrane system, two main forces are applied to the feed solution particles. The first one is the effective driving force (perpendicular to the membrane surface) dictated by the osmotic pressure difference between the feed and draw solutions, which causes the transfer of water molecules from the feed solution toward the draw solution side and forces the feed solution foulant particles to deposit on the membrane surface. The second one, which moves the feed solution molecules toward the bulk of the solution, is the shear force (moved tangentially to the membrane surface) caused by the CFV [51]. Applying ultrasound waves on the membrane active layer side generates other forces in the same direction of the system, driving forces that help in pushing the water molecules toward the draw solution side, which ultimately enhances water flux.

The increase in flux with the use of ultrasound at the membrane active layer side is in agreement with Heikkinen et al., who observed flux enhancement upon applying ultrasound on the CTA membrane active layer [28]. However, Heikkinen et al. [28] found better flux enhancement when the ultrasound source faced the membrane support layer. This is in contrary to the findings of this study. As shown in Figure 3, there is a decrease in the average water flux, compared to the baseline conditions, when using the ultrasound with the membrane support layer facing the draw solution for all the considered cases except the case of 1.0-CC-SL, which showed an increase of around 9.7%. For the case of 0.25-C-SL, the average flux decreased from 7.95 to 5.01 L/m^2·h, which represents 37.1% flux reduction. For the case of 1.0-C-SL and 0.25-CC-SL, the average water flux decreased from 14.44 and 6.57 L/m^2·h to 13.20 and 5.63 L/m^2·h, respectively, with respect to the baseline. The decrease in the water flux could be attributed to reverse solute flux caused by the application of the ultrasound toward the membrane support layer. Reverse solute flux promotes transfer of the solute from the draw solution toward the feed solution. This agrees with the findings of Qasim et al. [26] and Heikkinen et al. [28], who reported that the application of ultrasound on the membrane support layer increases the reverse solute flux. The reverse solute flux from the draw solution side toward the feed solution side complicates the fouling layer and worsens the ECP by trapping the draw solution solute particles between the membrane surface and the fouling layer, thus inducing the formation of an accelerated CEOP that causes a significant flux decline [44]. For this reason, the reverse solute flux did not reveal a significant change in the feed solution conductivity measurements, as shown in Figure 5. This figure shows representative examples of the relation between the measured and the estimated conductivity values during the time of the experiment. The estimated conductivity values were obtained through the application of mass balance on conductivity, assuming no solutes transfer occurs from the feed solution to the draw solution side (i.e., water molecules were only transferred). It should be noted

that NaCl shows a high potential for reverse solute flux due to its small ionic size [52,53]. Moreover, the turbulence zones and their associated forces generated by the ultrasound in the opposite direction of the water molecules transfer (from the feed to the draw solution) may also hinder the water transfer process, especially when the membrane active layer is exposed to fouling and ECP conditions. Applying ultrasound toward the support layer side would not have a powerful impact on reducing the formation of the fouling layer on the membrane active layer. On the contrary, weak ultrasound waves received at the active layer side could have caused the formed fouling layer to be denser and more spread on the surface, which negatively affected the membrane flux relative to the baseline conditions.

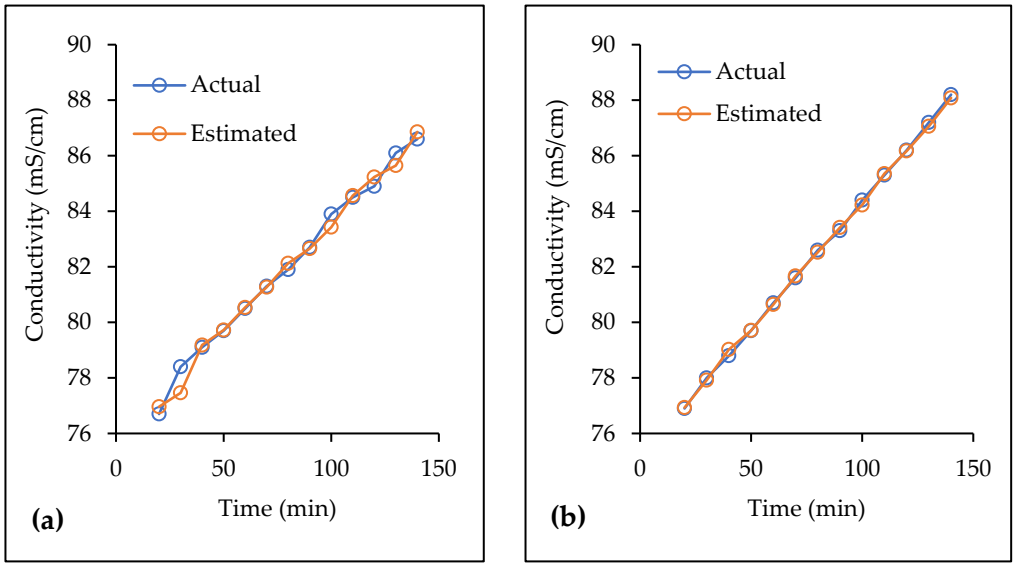

Figure 5. Measured and estimated conductivity values for NaCl draw solution for the case of (**a**) 0.25-C-AL (2nd run) and (**b**) 1.0-CC-SL (1st run).

The formation of a fouling thick gel layer and the ECP effect at the surface of the membrane active layer create an additional resistance to the system. Thus, considering the flow resistance created by the ultrasound effect in the opposite side (draw solution side), the available driving force (osmotic pressure difference) would not be adequate to overcome these resistances. This is consistent with the results observed for the cases of 0.25-C-SL and 0.25-CC-SL, where the effect of fouling is more severe at low CFV. For the case of 1.0-C-SL, the adverse effect of using ultrasound facing the support layer on the water flux was less pronounced compared to the case at low CFV (0.25-C-SL). It is possible that the high CFV minimizes the effect of fouling and ECP at the active layer, and it induces mixing at the support layer assisted by the impact of the ultrasound for minimizing the ICP [54], yet the flux was lower than the corresponding value obtained without the use of ultrasound (1.0-C-BL).

A water flux enhancement of around 9.7% was observed for the case of 1.0-CC-SL, where the average water flux increased from 12.51 L/m^2·h under baseline conditions to 12.73 L/m^2·h with the use of ultrasound (Figure 3). This is due to the combined effects of the ultrasound, the high CFV, and the counter-current flow configuration. The use of ultrasound minimizes the effect of ICP by mixing the produced permeate water with the draw solution that ultimately enhances the draw solution diffusion rate and, thus, increases the water flux [25]. The high CFV contributes to the low impact of resistance layers (fouling and ECP) and minimizes the mass transfer boundary layer (i.e., becomes thinner) at the membrane surface [55]. Moreover, using the counter-current configuration resulted in lowering the fouling effect at the membrane active layer surface [56]. In this case (1.0-CC-SL), it is expected that the combined effect of high CFV and counter-current flow configuration leads to reducing the system resistance and thus facilitates the effort of

the ultrasound in minimizing the ICP effect. Because of that, the system driving force was able to overcome the resistance produced by the ultrasound that was translated into flux enhancement.

3.1.3. Effect of CFV

The results for the effect of the CFV on the membrane flux for the different investigated cases are displayed in Table 3. It can be concluded (Table 3) that operating the system at higher velocity (1 cm/s) results in higher water flux. This is true for all the investigated cases. For the baseline conditions, increasing the CFV from 0.25 to 1.0 cm/s increases the average water flux from 7.95 to 14.44 L/m^2·h and from 6.57 to 12.51 L/m^2·h when using co-current and counter-current configurations, respectively. Moreover, the application of the ultrasound on the membrane active layer causes an increase in the average water flux from 10.66 to 14.97 L/m^2·h and from 11.22 to 15.16 L/m^2·h, resulting in an enhancement of 40.4% and 35.1% when using the co-current and counter-current configurations, respectively (Table 3). A flux enhancement of around 163.5% and 143.9% was observed by applying the ultrasound on the membrane support layer when using the co-current and counter-current configurations, respectively. The average flux increased from 5.01 to 13.2 L/m^2·h under co-current conditions and from 5.63 to 13.73 L/m^2·h under counter-current conditions.

Table 3. Average water flux (L/m^2·h) at low and high CFV for the investigated cases using NaCl draw solution.

Low CFV		High CFV		Flux Change (%)
Case	**Average J_w**	**Case**	**Average J_w**	
0.25-C-BL	7.95	1.0-C-BL	14.44	81.6
0.25-CC-BL	6.57	1.0-CC-BL	12.51	91.4
0.25-C-AL	10.66	1.0-C-AL	14.97	40.4
0.25-CC-AL	11.22	1.0-CC-AL	15.16	35.1
0.25-C-SL	5.01	1.0-C-SL	13.2	163.5
0.25-CC-SL	5.63	1.0-CC-SL	13.73	143.9

The increase in water flux due to the increase in the CFV can be attributed to the decrease in the mass transfer boundary layer thickness at the membrane surface, which leads to an increase in the mass transfer rate that causes flux enhancement [55]. In addition, the high CFV minimizes the rate of the fouling layer and enhances the removal of the formed fouling layer on the membrane surface (due to the shear force) [57]. The high CFV also minimizes the effect of the ECP that limits the water flux and induces a mixing effect, assisted by the ultrasound, at the membrane support layer to decrease the impact of ICP that increases the water flux [54]. The high flux enhancement upon moving from a low to a high CFV with the ultrasound facing the support layer (Table 3) supports the conjecture that using ultrasound at the support layer induces mixing and turbulent zones and, thus, lowers the impact of ICP and enhances the water flux. This is consistent with the findings of Choi et al. [25], who found that using a low-frequency ultrasound source could significantly decrease the ICP effect and cause a higher membrane flux enhancement.

3.1.4. Effect of Flow Configuration

The results for the effect of flow patterns on the membrane flux for the different configurations (co-current versus counter-current) used in this work are shown in Table 4. Changing from a co-current to a counter-current configuration causes the average water flux to decrease 17.4% and 13.4% for the baseline cases at low and high CFV, respectively. This trend could be due to the differences in the features of the co-current and the counter-current configurations. In the co-current configuration, the osmotic pressure difference (between the feed and draw solutions) at the beginning of the testing cell is high, which provides a high initial flux that gradually decreases along the membrane length [52]. Considering the fouling layer formation at the membrane active layer surface, the high osmotic pressure

difference helps the water molecules to transfer from the feed to the draw solution by providing flow capable of overcoming the resistance of the fouling layer at the active layer side. Thus, the implementation of a co-current configuration in the absence of ultrasound waves resulted in a slightly higher water flux than the counter-current one.

Table 4. Effects of flow configuration on the average water flux (L/m^2·h) using NaCl draw solution.

Co-Current Flow		Counter-Current Flow		Flux Change (%)
Case	Average J_w	Case	Average J_w	
0.25-C-BL	7.95	0.25-CC-BL	6.57	−17.4
1.0-C-BL	14.44	1.0-CC-BL	12.51	−13.4
0.25-C-AL	10.66	0.25-CC-AL	11.22	5.25
1.0-C-AL	14.97	1.0-CC-AL	15.16	1.3
0.25-C-SL	5.01	0.25-CC-SL	5.63	12.4
1.0-C-SL	13.20	1.0-CC-SL	13.73	4.0

It should be noted that the counter-current flow configuration provides almost a uniform flux due to the nearly constant osmotic pressure difference between the feed and draw solutions, which ultimately minimizes the fouling effect. However, this is highly dependent on the feed solution characteristics and the system operating conditions [56]. This may explain the minor effect of the counter-current configuration on flux enhancement in the presence of the ultrasound (i.e., the ultrasound effect in minimizing the fouling is dominant and more effective than the counter-current flow configuration).

3.2. Effect of $MgCl_2$ as a Draw Solution

Tests similar to those conducted using NaCl draw solution in the previous section were also performed using $MgCl_2$ in order to determine the membrane performance due to the presence of divalent ions in the draw solution. Following the same conditions, baseline tests (without the use of ultrasound) and with the use of ultrasound for $MgCl_2$ were conducted, and the membrane average water flux results are shown in Figure 6.

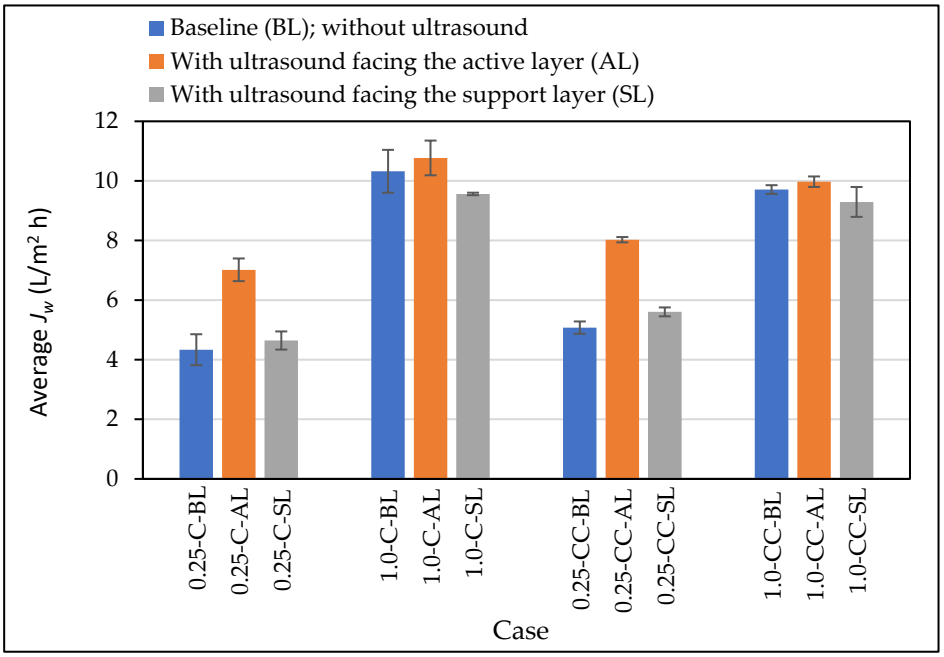

Figure 6. Average J_w for the cases with and without the use of ultrasound for $MgCl_2$ draw solution. The error bar represents the lower and upper average J_w associated with the two runs of the tested case.

3.2.1. Baseline Conditions

Generally, the water flux without the use of ultrasound increases with the increase in the CFV for both flow configurations (Figure 6). Increasing the CFV from 0.25 to 1.0 cm/s resulted in an increase in the water flux by 138.1% (from 4.33 to 10.32 L/m^2·h) and 91.3% (from 5.08 to 9.71 L/m^2·h) when using co-current and counter-current configurations, respectively. The highest water flux was observed for the case of 1.0-C-BL with an average value of 10.32 L/m^2·h, while the flux for the case of 0.25-C-BL was the lowest at 4.33 L/m^2·h. Figure 6 shows that at a CFV of 0.25 cm/s and without the use of ultrasound, the average water flux increases from 4.33 with co-current flow to 5.08 L/m^2·h with counter-current flow. However, the average water flux decreases from 10.32 with co-current flow to 9.71 L/m^2·h with counter-current flow at a CFV of 1.0 cm/s. Similar to the approach used when NaCl was deployed as a draw solution, the above water flux values will be considered as baselines to assess the effect of using ultrasound on the membrane flux performance with $MgCl_2$ as a draw solution.

3.2.2. Effect of Ultrasound on Membrane Performance

The effect of applying ultrasound on the membrane average water flux was investigated using similar configurations as those used for the NaCl solution, namely 0.25-C-AL, 1.0-C-AL, 0.25-CC-AL, 1.0-CC-AL, 0.25-C-SL, 1.0-C-SL, 0.25-CC-SL, and 1.0-CC-SL. The average water fluxes for such configurations, in the absence (baseline conditions) and the presence of the ultrasound, are shown in Figure 6. For all cases, the water flux increases in the presence of ultrasound, except for the two cases of 1.0-C-SL and 1.0-CC-SL, where the water flux is slightly lower than that of the baseline value.

As demonstrated in Figure 6, the most significant water flux enhancement was observed for the case of 0.25-C-AL, where the average flux increased from 4.33 L/m^2·h under the baseline conditions to 7.02 L/m^2·h when the ultrasound was deployed. For the 0.25-CC-AL case, an average water flux of 5.08 L/m^2·h was observed under the baseline conditions, which increased to 8.03 L/m^2·h with the use of ultrasound (i.e., 58.1% flux enhancement). Using the ultrasound in the cases of 1.0-C-AL and 1.0-CC-AL resulted in a slight improvement (<5%) in the average water flux with the use of ultrasound, which could be considered insignificant given the overlap between the range of the average water flux with and without the use of ultrasound for each case.

Having the ultrasound source facing the membrane active layer significantly enhanced the average water flux at low CFV. This is consistent with what was observed when NaCl was used as the draw solution and could be attributed to the formation of a fouling layer and the ECP that were more severe at the low CFV under baseline conditions. It seems that the use of the ultrasound source at the membrane active layer decreased the formation of these layers, which was ultimately reflected in the membrane water flux improvement. It was also observed that the effect of the ultrasound on the water flux at the high CFV (1.0 cm/s) was insignificant compared to the results observed at low CFV (0.25 cm/s). This could be due to the effect of the high CFV assisted by the ultrasound on cleaning the membrane surface and its role in minimizing the ECP effect. Generally, changing the flow configuration (co-current or counter-current) when the ultrasound source faces the active layer showed a low effect on flux enhancement, which is consistent with the previous findings for the cases conducted with NaCl as a draw solution.

Based on the above, and because all the tests for the NaCl and $MgCl_2$ draw solutions were conducted at similar conditions, including the presence of fouling and scaling substances in the feed solution, the membrane active layer surface with $MgCl_2$ as a draw solution is also exposed to fouling and concentration polarization problems. As such, the previously discussed fouling and concentration polarization mechanisms can also be applied to the cases where $MgCl_2$ is used as a draw solution. However, considering the use of $MgCl_2$ as a draw solution, the membrane surface is expected to experience severe fouling issues due to the possibility of reverse solute flux from the draw solution to the feed solution side, which would make the characteristics of the formed fouling layer more

complicated due to possible interaction of Mg^{2+} ions with the components of the feed solution [58]. Thus, despite the advantages associated with the use of a multivalent ion draw solution with a larger ion size that minimizes reverse solute flux, the process of reverse solute flux cannot be totally ignored [53].

The use of ultrasound in the presence of $MgCl_2$ as a draw solution caused an improvement in the membrane average water flux, which was similar when NaCl was used as a draw solution. This is due to the ability of the ultrasound waves to decrease the system overall resistance by minimizing the ECP effect and decrease the external fouling layer effect by breaking the formed layer and detaching the deposited foulants on the membrane active layer surface.

The results in Figure 6 indicate that the application of ultrasound on the membrane support layer has a slight or insignificant impact on the average water flux. For the cases at low CFV (0.25-C-SL and 0.25-CC-SL), the average water flux, compared to the baseline conditions, increased from 4.33 to 4.64 L/m^2·h and from 5.08 to 5.61 L/m^2·h, respectively, i.e., around 7.1% (0.25-C-SL) and 10.5% (0.25-CC-SL) flux improvement. For the cases of 1.0-C-SL and 1.0 -CC-SL, the average flux decreased from 10.32 and 9.71 L/m^2·h (under the baseline conditions) to 9.56 L/m^2·h and 9.29 L/m^2·h, respectively, i.e., about 7.4% (1.0-C-SL) and 4.3% (1.0-CC-SL) flux reduction.

The observed decrease in the average water flux at the high CFV could be due to the impact of reverse solute flux that may transfer the draw solution solute particles from the draw solution to the feed solution side. This reverse solute flux increases by increasing the CFV [59,60] and decreasing the impact of the ICP [42]. Therefore, the application of the ultrasound on the membrane support layer decreased the ICP effect at the membrane support layer [26] and simultaneously increased the chances for reverse solute particles ($MgCl_2$) to transfer from the draw solution to the feed solution side [26,28]. As such, the reverse solute flux could affect the fouling layer formed at the membrane active layer, where the draw solution particles (Mg^{2+}) may become trapped between the membrane surface and the fouling layer and, thus, interact with the feed solution substances such as alginate, making the ECP and fouling effects more pronounced [42,58]. It is noted that the reverse solute flux did not cause a significant increase in the feed solution conductivity measurements. This promotes the formation of the accelerated CEOP that causes a significant decrease in the flux due to the system high resistance and the decrease in the net osmotic pressure driving force [44]. Moreover, the use of ultrasound could also minimize the impact of dilution of the draw solution that would ultimately increase the concentration gradient and, thus, promote the reverse solute flux from the draw toward the feed solution [26]. This can also explain the observed flux enhancement under low CFV. Low CFV could minimize reverse solute transfer from the draw to the feed solution and, thus, minimize the fouling layer effect that ultimately increases the water flux. This agrees with the findings of Zou et al. [58], who reported that the use of $MgCl_2$ as a draw solution can cause a severe FO membrane fouling problem due to the reverse solute flux of magnesium ions toward the feed solution and their interaction with the algae substances presented in the feed solution, which results in a water flux reduction.

3.2.3. Effect of CFV

The results for the effect of the CFV on the membrane water flux for the different configurations using $MgCl_2$ as a draw solution are shown in Table 5. Operating the system at higher CFV (1 cm/s) reveals higher water flux in all testing configurations (Table 5). Under baseline conditions, increasing the CFV from 0.25 to 1.0 cm/s increases the average water flux from 4.33 to 10.32 L/m^2·h for the co-current configuration and from 5.08 to 9.71 L/m^2·h for the counter-current configuration, which represents a flux enhancement of 138.3% and 91.1%, respectively (Table 5). Moreover, the application of the ultrasound on the membrane active layer causes a flux enhancement, relative to the baseline conditions, of 53.4% and 24.2% for the co-current and the counter-current configurations, respectively (Table 5). A flux enhancement of 106.0% and 65.6% was observed by applying

the ultrasound on the membrane support layer when using the co-current and the counter-current configurations, respectively. Similar to the interpretation made with the NaCl as a draw solution, the increase in water flux due to the increase in the CFV can be attributed to the decrease in the mass transfer boundary layer thickness at the membrane surface. The increase in the CFV resulted in a decrease in the mass transfer boundary layer thickness (becomes thinner), which led to an increase in the mass transfer rate that is ultimately reflected in the flux enhancement [55]. In addition, the high CFV minimizes the formation rate of the fouling layer and, thus, enhances the removal of the formed fouling layer on the membrane surface (due to the shear force) [58]. Meanwhile, high CFV minimizes the effect of the ECP that limits the water flux and induces a mixing effect, assisted by the applied ultrasound, at the membrane support layer to decrease the ICP effect, which increases the water flux [13,54]. Based on the results presented in Table 5, the high flux enhancement observed upon moving from a low to a high CFV with the ultrasound facing the support layer supports the conclusion previously made for the NaCl part, i.e., application of the ultrasound at the support layer induces mixing and turbulent zones that decrease the impact of ICP and enhance the water flux.

Table 5. Average water flux ($L/m^2 \cdot h$) at low and high CFV for the cases with $MgCl_2$ draw solution.

Low CFV		High CFV		Flux Change (%)
Case	**Average J_w**	**Case**	**Average J_w**	
0.25-C-BL	4.33	1.0-C-BL	10.32	138.3
0.25-CC-BL	5.08	1.0-CC-BL	9.71	91.1
0.25-C-AL	7.02	1.0-C-AL	10.77	53.4
0.25-CC-AL	8.03	1.0-CC-AL	9.97	24.2
0.25-C-SL	4.64	1.0-C-SL	9.56	106.0
0.25-CC-SL	5.61	1.0-CC-SL	9.29	65.6

3.2.4. Effect of Flow Configuration

The results for the effects of flow patterns on the membrane flux for different configurations using $MgCl_2$ as a draw solution are displayed in Table 6. At low CFV, changing flow configuration from co-current to counter-current causes an increase in the average water flux of 14.4–20.9%. This is due to the features of the counter-current configuration that minimizes the fouling effect (due to the osmotic pressure difference behavior between the feed and draw solutions within the testing cell) [52] in conjunction with the low CFV that minimizes the reverse solute effect, which reduces the system overall resistance and thus increases the membrane water flux.

Table 6. Effects of flow configuration on the average water flux ($L/m^2 \cdot h$) using $MgCl_2$ draw solution.

Co-Current Flow		Counter-Current Flow		Flux Change (%)
Case	**Average J_w**	**Case**	**Average J_w**	
0.25-C-BL	4.33	0.25-CC-BL	5.08	17.3
1.0-C-BL	10.32	1.0-CC-BL	9.71	−5.9
0.25-C-AL	7.02	0.25-CC-AL	8.03	14.4
1.0-C-AL	10.77	1.0-CC-AL	9.97	−7.4
0.25-C-SL	4.64	0.25-CC-SL	5.61	20.9
1.0-C-SL	9.56	1.0-CC-SL	9.29	−2.8

At high CFV, the average water flux slightly decreased by 2.8–7.42% due to changes from a co-current to a counter-current configuration. The difference in water flux between the co-current and counter-current configurations could be due to the features of the co-current configuration, where the osmotic pressure difference (between the feed and draw solutions) at the beginning of the process is high, providing a high initial flux that gradually decreases along the membrane length [52]. The high initial osmotic pressure difference

helps the water molecules to transfer from the feed to the draw solution by providing flow capable to overcome the resistance of the fouling layer at the active layer side. Thus, the co-current configuration revealed a slightly higher water flux than the counter-current configuration. The counter-current flow configuration may provide almost a uniform flux due to the nearly constant osmotic pressure difference between the feed and draw solutions, which ultimately minimizes the fouling effect. However, this is strongly dependent on the feed solution characteristics and the system operating conditions [56,61].

3.3. Comparison of Flux Produced by NaCl and $MgCl_2$ Draw Solutions

Since the draw solution is considered the main driving force in the FO process that dictates the membrane water flux, its type (monovalent or divalent) plays an important role in the process performance. As such, the draw solution needs to be capable of generating higher osmotic pressure than the one in the feed solution to facilitate transfer of the water molecules from the feed solution toward the draw solution. Since the selected concentrations for NaCl and $MgCl_2$ in this study provide almost similar initial osmotic pressure values [33], it is possible to compare between the water flux produced from each type.

Under the baseline conditions, the use of NaCl as a draw solution resulted in a higher water flux compared to that of $MgCl_2$ (Figure 7a). The respective average water flux (in $L/m^2.h$) produced using NaCl and $MgCl_2$ draw solutions for the baseline cases is 7.95 and 4.33 for the case 0.25-C-BL, 14.44 and 10.32 for 1.0-C-BL, 6.57 and 5.08 for 0.25-CC-BL, and 12.51 and 9.71 for 1.0-CC-BL (Figures 3 and 6). Using NaCl as a draw solution against $MgCl_2$ provides an average water flux increase of 83.5% (0.25-C-BL), 39.9% (1.0-C-BL), 29.4% (0.25-CC-BL), and 28.9% (1.0-CC-BL) (Figure 7a).

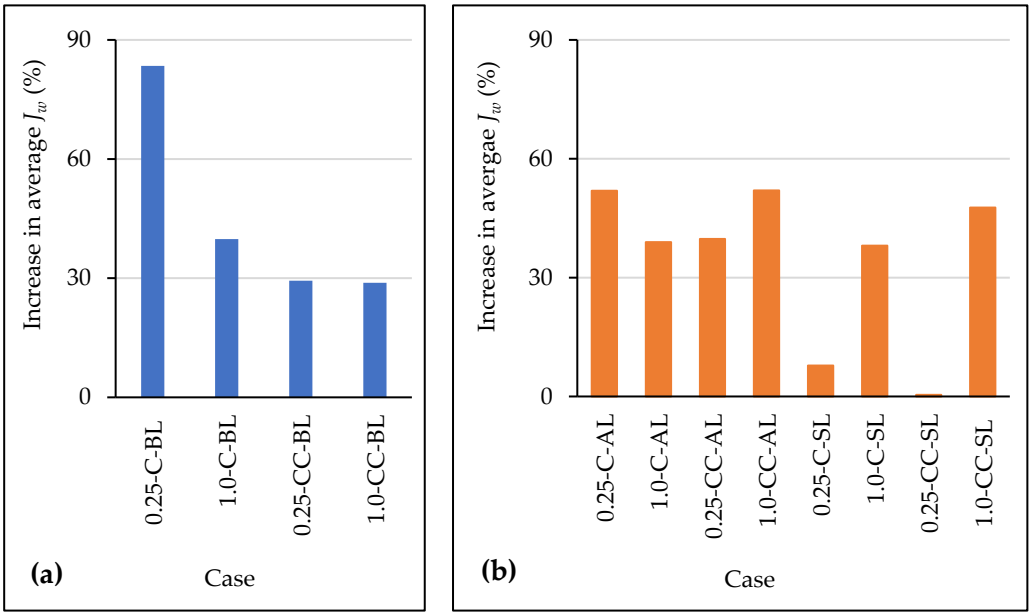

Figure 7. Increase in average J_w using NaCl compared to $MgCl_2$ draw solution (**a**) without the use of ultrasound and (**b**) with the use of ultrasound.

In the presence of ultrasound, the use of NaCl draw solution reveals higher water flux values than the ones observed with the use of $MgCl_2$ for almost all the investigated cases in this work (Figure 7b). However, no significant water flux enhancement was observed for the case 0.25-CC-SL, where the average water flux shows an insignificant improvement of 0.3% (5.63 $L/m^2{\cdot}h$ with the case of NaCl and 5.61 $L/m^2{\cdot}h$ with the case of $MgCl_2$). At high CFV, the highest average water flux (15.16 $L/m^2{\cdot}h$) was obtained for the case of 1.0-CC-AL with NaCl draw solution, while the lowest flux (9.29 $L/m^2{\cdot}h$) occurred for the case of 1.0-CC-SL with $MgCl_2$ draw solution. At low CFV, a maximum average water flux value of

11.22 L/m^2·h was obtained when using 0.25-CC-AL with NaCl draw solution, while the lowest flux (4.64 L/m^2·h) was observed when using 0.25-C-SL with $MgCl_2$ draw solution.

The observed flux enhancement using NaCl as a draw solution compared to the one for $MgCl_2$ is mainly attributed to the characteristics associated with the NaCl of having a higher diffusivity, lower viscosity, and lower molecular weight than those of $MgCl_2$ [62]. The smaller ionic size associated with NaCl allows for better solute dispersion within the solution. This provides a higher diffusion rate that minimizes the system overall resistance and reduces the effect of the ICP, which ultimately enhances the water flux [13]. This is consistent with the findings of Achilli et al. [11], who reported that at the same osmotic pressure, the flux produced by NaCl draw solution is higher than the one produced by $MgCl_2$.

The highly diffused NaCl draw solution into the membrane support layer resulted in a decrease in the respective system ICP and, thus, caused an increase in the membrane water flux [52]. However, the small molecular size associated with the NaCl leads to an increase in the reverse solute flux and, thus, worsens the fouling effect [13]. Therefore, the use of $MgCl_2$ as a draw solution would minimize the effect of reverse solute flux due to the large size of the ions and their low diffusion properties [11,33]. It should be highlighted that using $MgCl_2$ promotes the impact of ICP within the membrane support layer that causes an adverse effect on the water flux [63]. Therefore, the application of the ultrasound minimizes the effect of the ICP and enhances the membrane water flux. However, using ultrasound promotes the reverse solute flux, which influences the fouling layer characteristics and the system concentration polarization that leads to a flux reduction. Therefore, special attention needs to be considered in using the ultrasound toward the support layer to avoid any adverse effect on the membrane performance.

3.4. Suggested Future Work

This study explored the effect of some of the operating parameters of ultrasound-assisted FO system on water flux enhancement for water desalination. Several other parameters that could affect the system performance have not been addressed including changes in the ultrasound frequency and power, the use of ultrasound intermittent mode, and the use of other values of CFV. Our results showed that CFV is a significant factor that affects the performance of the system, but no attempt was devoted to find the optimum CFV. Moreover, previous studies showed that ultrasound frequency and power are also significant factors for flux enhancement [25]. In addition, flux enhancement was higher with pulse ultrasound as compared with a continuous one [28].

A fixed concentration of the scalant and foulant materials was applied to the feed solution in this study. The concentration of the scalant and the foulant is expected to have a major impact on water flux. To better understand the role of scalant and foulant material on the performance of ultrasound-assisted FO systems, future studies may consider varying the concentration of these materials with consideration of testing their individual as well as their combined impact.

One of the limitations of this study is the lack of analysis of the deposit material that is formed on the active layer of the membrane, making our interpretations rather speculative. To confirm that, efforts should be devoted to relate the changes in the water flux through the membrane in ultrasound-assisted FO systems with the nature, characteristics, amount, and distribution of the deposit material on the membrane layer.

In this study, a concern was raised regarding reverse solute flux from the draw solution to the feed solution side that is caused by using the ultrasound toward the membrane support layer. Taking this into consideration and to maximize the benefits obtained from the advantages associated with the individual type of the draw solutions (NaCl and $MgCl_2$), it is recommended to study the effect of the ultrasound on the FO membrane performance using a mixed draw solution (NaCl + $MgCl_2$).

4. Conclusions

The application of a continuous ultrasound frequency of 40 kHz is effective in enhancing the water flux through the FO membrane, especially when the ultrasound source faces the membrane active layer. This applies to both types of the used draw solutions, namely NaCl and $MgCl_2$. With the use of NaCl as a draw solution, the highest water flux enhancement (70.8%) was found at the low flow velocity, with a counter-current flow, and the ultrasound facing the membrane active layer. For the case in which $MgCl_2$ was the draw solution, the highest flux enhancement 61.9% occurred at low flow velocity, with a co-current flow, and the ultrasound facing the active layer. However, using ultrasound resulted in slight flux enhancement or caused an adverse effect on water flux when it faced the membrane support layer. Using the ultrasound toward the membrane support layer increased the reverse solute flux from the draw solution to the feed solution side that enhanced the formation of an accelerated cake-enhanced osmotic pressure fouling layer and amplified the external concentration polarization. This was found to be more pronounced with the use of NaCl as compared to the use of $MgCl_2$ as a draw solution. The application of ultrasound toward the membrane support layer needs to be carefully studied, taking into consideration the feed solution characteristics. Moreover, draw solutions with monovalent ions (such as NaCl) outperformed those with divalent ions ($MgCl_2$) in terms of water flux enhancement in all tested cases.

Supplementary Materials: The following supplementary information can be downloaded at: https://www.mdpi.com/article/10.3390/w14132092/s1, Table S1: Flux and feed solution conductivity for the experiments with NaCl draw solution without ultrasound; Table S2: Flux and feed solution conductivity for the experiments with NaCl draw solution with ultrasound; Table S3: Flux and feed solution conductivity for the experiments with $MgCl_2$ draw solution without ultrasound; Table S4: Flux and feed solution conductivity for the experiments with $MgCl_2$ draw solution with ultrasound.

Author Contributions: Conceptualization, B.A.K.A.-S. and S.A.-A.; methodology, B.A.K.A.-S. and S.A.-A.; validation, B.A.K.A.-S., S.A.-A. and M.A.M.; formal analysis, B.A.K.A.-S.; investigation, B.A.K.A.-S.; resources, S.A.-A. and M.A.M.; data curation, B.A.K.A.-S.; writing—original draft preparation, B.A.K.A.-S.; writing—review and editing, S.A.-A. and M.A.M.; visualization, B.A.K.A.-S. and M.A.M.; supervision, S.A.-A. and M.A.M.; project administration, M.A.M.; funding acquisition, M.A.M. All authors have read and agreed to the published version of the manuscript.

Funding: This research received no external funding.

Institutional Review Board Statement: Not applicable.

Informed Consent Statement: Not applicable.

Data Availability Statement: Not applicable.

Acknowledgments: Partial support for this study was provided by the College of Engineering at the United Arab Emirates University. The authors also acknowledge the support of the College of Engineering at the American University of Sharjah, namely the guidance of Ahmad Aidan and Mohamad Qasim in the experimental setup.

Conflicts of Interest: The authors declare no conflict of interest.

References

1. Qasim, M.; Badrelzaman, M.; Darwish, N.N.; Darwish, N.A.; Hilal, N. Reverse osmosis desalination: A state-of-the-art review. *Desalination* **2019**, *459*, 59–104. [CrossRef]
2. Eke, J.; Yusuf, A.; Giwa, A.; Sodiq, A. The global status of desalination: An assessment of current desalination technologies, plants and capacity. *Desalination* **2020**, *495*, 114633. [CrossRef]
3. IDA (International Desalination Association). Dynamic Growth for Desalination and Water Reuse in 2019. Available online: https://idadesal.org/dynamic-growth-for-desalination-and-water-reuse-in-2019/ (accessed on 9 August 2020).
4. Altaee, A.; Zaragoza, G.; van Tonningen, H.R. Comparison between forward osmosis-reverse osmosis and reverse osmosis processes for seawater desalination. *Desalination* **2014**, *336*, 50–57. [CrossRef]
5. Alnaizy, R.; Aidan, A.; Qasim, M. Copper sulfate as draw solute in forward osmosis desalination. *J. Environ. Chem. Eng.* **2013**, *1*, 424–430. [CrossRef]

6. Yen, S.K.; Mehnas Haja, N.F.; Su, M.; Wang, K.Y.; Chung, T.-S. Study of draw solutes using 2-methylimidazole-based compounds in forward osmosis. *J. Membr. Sci.* **2010**, *364*, 242–252. [CrossRef]
7. Ge, Q.; Su, J.; Amy, G.L.; Chung, T.-S. Exploration of polyelectrolytes as draw solutes in forward osmosis processes. *Water Res.* **2012**, *46*, 1318–1326. [CrossRef]
8. Zhao, S.; Zou, L.; Mulcahy, D. Brackish water desalination by a hybrid forward osmosis–nanofiltration system using divalent draw solute. *Desalination* **2012**, *284*, 175–181. [CrossRef]
9. Tan, C.H.; Ng, H.Y. A novel hybrid forward osmosis-nanofiltration (FO-NF) process for seawater desalination: Draw solution selection and system configuration. *Desalination Water Treat.* **2010**, *13*, 356–361. [CrossRef]
10. Yangali-Quintanilla, V.; Li, Z.; Valladares, R.; Li, Q.; Amy, G. Indirect desalination of Red Sea water with forward osmosis and low pressure reverse osmosis for water reuse. *Desalination* **2011**, *280*, 160–166. [CrossRef]
11. Achilli, A.; Cath, T.Y.; Childress, A.E. Selection of inorganic-based draw solutions for forward osmosis applications. *J. Membr. Sci.* **2010**, *364*, 233–241. [CrossRef]
12. Voutchkov, N. Energy use for membrane seawater desalination—Current status and trends. *Desalination* **2018**, *431*, 2–14. [CrossRef]
13. Suwaileh, W.; Pathak, N.; Shon, H.; Hilal, N. Forward osmosis membranes and processes: A comprehensive review of research trends and future outlook. *Desalination* **2020**, *485*, 114455. [CrossRef]
14. Li, L.; Shi, W.; Yu, S. Research on forward osmosis membrane technology still needs improvement in water recovery and wastewater treatment. *Water* **2019**, *12*, 107. [CrossRef]
15. Haupt, A.; Lerch, A. Forward osmosis application in manufacturing industries: A short review. *Membranes* **2018**, *8*, 47. [CrossRef] [PubMed]
16. WaterWorld. Getting to Know the Forward Osmosis Pioneer. Available online: https://www.waterworld.com/technologies/article/16201806/getting-to-know-the-forward-osmosis-pioneer (accessed on 9 August 2020).
17. Modern Water Commissions Al Najdah FO Plant. *Membr. Technol.* **2012**, *2012*, 4. [CrossRef]
18. Qasim, M.; Mohammed, F.; Aidan, A.; Darwish, N.A. Forward osmosis desalination using ferric sulfate draw solute. *Desalination* **2017**, *423*, 12–20. [CrossRef]
19. Xu, Y.; Peng, X.; Tang, C.Y.; Fu, Q.S.; Nie, S. Effect of draw solution concentration and operating conditions on forward osmosis and pressure retarded osmosis performance in a spiral wound module. *J. Membr. Sci.* **2010**, *348*, 298–309. [CrossRef]
20. Qasim, M.; Darwish, N.A.; Sarp, S.; Hilal, N. Water desalination by forward (direct) osmosis phenomenon: A comprehensive review. *Desalination* **2015**, *374*, 47–69. [CrossRef]
21. Lee, W.J.; Ng, Z.C.; Hubadillah, S.K.; Goh, P.S.; Lau, W.J.; Othman, M.H.D.; Ismail, A.F.; Hilal, N. Fouling mitigation in forward osmosis and membrane distillation for desalination. *Desalination* **2020**, *480*, 114338. [CrossRef]
22. Qasim, M.; Darwish, N.N.; Mhiyo, S.; Darwish, N.A.; Hilal, N. The use of ultrasound to mitigate membrane fouling in desalination and water treatment. *Desalination* **2018**, *443*, 143–164. [CrossRef]
23. Chanukya, B.S.; Rastogi, N.K. Ultrasound assisted forward osmosis concentration of fruit juice and natural colorant. *Ultrason. Sonochem.* **2017**, *34*, 426–435. [CrossRef] [PubMed]
24. Nguyen, N.C.; Nguyen, H.T.; Chen, S.-S.; Nguyen, N.T.; Li, C.-W. Application of forward osmosis (FO) under ultrasonication on sludge thickening of waste activated sludge. *Water Sci. Technol.* **2015**, *72*, 1301–1307. [CrossRef] [PubMed]
25. Choi, Y.; Hwang, T.-M.; Jeong, S.; Lee, S. The use of ultrasound to reduce internal concentration polarization in forward osmosis. *Ultrason. Sonochem.* **2018**, *41*, 475–483. [CrossRef] [PubMed]
26. Qasim, M.; Khudhur, F.W.; Aidan, A.; Darwish, N.A. Ultrasound-assisted forward osmosis desalination using inorganic draw solutes. *Ultrason. Sonochem.* **2020**, *61*, 104810. [CrossRef]
27. Kim, H.; Lee, Y.; Elimelech, M.; Adout, A.; Kim, Y.C. Experimental Study of Ultrasonic Effects on Flux Enhancement in Forward Osmosis Process. The Electrochemical Society, Meeting Abstract MA2012-01 90. 2012. Available online: https://iopscience.iop.org/article/10.1149/MA2012-01/4/90/pdf (accessed on 1 May 2022).
28. Heikkinen, J.; Kyllönen, H.; Järvelä, E.; Grönroos, A.; Tang, C.Y. Ultrasound-assisted forward osmosis for mitigating internal concentration polarization. *J. Membr. Sci.* **2017**, *528*, 147–154. [CrossRef]
29. Choi, Y.-J.; Kim, S.-H.; Jeong, S.; Hwang, T.-M. Application of ultrasound to mitigate calcium sulfate scaling and colloidal fouling. *Desalination* **2014**, *336*, 153–159. [CrossRef]
30. Kim, Y.; Li, S.; Ghaffour, N. Evaluation of different cleaning strategies for different types of forward osmosis membrane fouling and scaling. *J. Membr. Sci.* **2020**, *596*, 117731. [CrossRef]
31. Chen, S.C.; Su, J.; Fu, F.-J.; Mi, B.; Chung, T.-S. Gypsum ($CaSO_4 \cdot 2H_2O$) scaling on polybenzimidazole and cellulose acetate hollow fiber membranes under forward osmosis. *Membranes* **2013**, *3*, 354–374. [CrossRef]
32. Mi, B.; Elimelech, M. Chemical and physical aspects of organic fouling of forward osmosis membranes. *J. Membr. Sci.* **2008**, *320*, 292–302. [CrossRef]
33. Cath, T.; Childress, A.; Elimelech, M. Forward osmosis: Principles, applications, and recent developments. *J. Membr. Sci.* **2006**, *281*, 70–87. [CrossRef]
34. Ge, Q.; Ling, M.; Chung, T.S. Draw solutions for forward osmosis processes: Developments, challenges, and prospects for the future. *J. Membr. Sci.* **2013**, *442*, 225–237. [CrossRef]

35. Loeb, S.; Titelman, L.; Korngold, E.; Freiman, J. Effect of porous support fabric on osmosis through a Loeb-Sourirajan type asymmetric membrane. *J. Membr. Sci.* **1997**, *129*, 243–249. [CrossRef]
36. Xu, W.; Chen, Q.; Ge, Q. Recent advances in forward osmosis (FO) membrane: Chemical modifications on membranes for FO processes. *Desalination* **2017**, *419*, 101–116. [CrossRef]
37. Corzo, B.; de la Torre, T.; Sans, C.; Ferrero, E.; Malfeito, J.J. Evaluation of draw solutions and commercially available forward osmosis membrane modules for wastewater reclamation at pilot scale. *Chem. Eng. J.* **2017**, *326*, 1–8. [CrossRef]
38. Phuntsho, P.; Hong, S.; Elimelech, M.; Shon, H.K. Forward osmosis desalination of brackish groundwater: Meeting water quality requirements for fertigation by integrating nanofiltration. *J. Membr. Sci.* **2013**, *436*, 1–15. [CrossRef]
39. Liu, Y.; Mi, B. Combined fouling of forward osmosis membranes: Synergistic foulant interaction and direct observation of fouling layer formation. *J. Membr. Sci.* **2012**, *407–408*, 136–144. [CrossRef]
40. Charfi, A.; Jang, H.; Kim, J. Membrane fouling by sodium alginate in high salinity conditions to simulate biofouling during seawater desalination. *Bioresour. Technol.* **2017**, *240*, 106–114. [CrossRef]
41. Linares, R.V.; Li, Z.; Yangali-Quintanilla, V.; Li, Q.; Vrouwenvelder, J.S.; Amy, G.L.; Ghaffour, N. Hybrid SBR–FO system for wastewater treatment and reuse: Operation, fouling and cleaning. *Desalination* **2016**, *393*, 31–38. [CrossRef]
42. She, Q.; Wang, R.; Fane, A.G.; Tang, C.Y. Membrane fouling in osmotically driven membrane processes: A review. *J. Membr. Sci.* **2016**, *499*, 201–233. [CrossRef]
43. Xie, M.; Lee, J.; Nghiem, L.D.; Elimelech, M. Role of pressure in organic fouling in forward osmosis and reverse osmosis. *J. Membr. Sci.* **2015**, *493*, 748–754. [CrossRef]
44. Lee, S.; Boo, C.; Elimelech, M.; Hong, S. Comparison of fouling behavior in forward osmosis (FO) and reverse osmosis (RO). *J. Membr. Sci.* **2010**, *365*, 34–39. [CrossRef]
45. Aghapour Aktij, S.; Taghipour, A.; Rahimpour, A.; Mollahosseini, A.; Tiraferri, A. A critical review on ultrasonic-assisted fouling control and cleaning of fouled membranes. *Ultrasonics* **2020**, *108*, 106228. [CrossRef] [PubMed]
46. Yasui, K. Acoustic Cavitation. In *Acoustic Cavitation and Bubble Dynamics*; Yasui, K., Ed.; Springer International Publishing: Cham, Switzerland, 2018; pp. 1–35. [CrossRef]
47. Chen, D.; Sharma, S.K.; Mudhoo, A. *Handbook on Applications of Ultrasound: Sonochemistry for Sustainability*, 1st ed.; CRC Press: Boca Raton, FL, USA, 2011.
48. Wu, T.Y.; Guo, N.; Teh, C.Y.; Hay, J.X.W. *Advances in Ultrasound Technology for Environmental Remediation*; Springer: Dordrecht, The Netherlands, 2013. [CrossRef]
49. Córdova, A.; Astudillo-Castro, C.; Ruby-Figueroa, R.; Valencia, P.; Soto, C. Recent advances and perspectives of ultrasound assisted membrane food processing. *Food Res. Int.* **2020**, *133*, 109163. [CrossRef]
50. Lamminen, M.O.; Walker, H.W.; Weavers, L.K. Mechanisms and factors influencing the ultrasonic cleaning of particle-fouled ceramic membranes. *J. Membr. Sci.* **2004**, *237*, 213–223. [CrossRef]
51. Chia, W.Y.; Khoo, K.S.; Chia, S.R.; Chew, K.W.; Yew, G.Y.; Ho, Y.-C.; Show, P.L.; Chen, W.-H. Factors affecting the performance of membrane osmotic processes for bioenergy development. *Energies* **2020**, *13*, 481. [CrossRef]
52. Cai, Y.; 'Matthew' Hu, X. A critical review on draw solutes development for forward osmosis. *Desalination* **2016**, *391*, 16–29. [CrossRef]
53. Alejo, T.; Arruebo, M.; Carcelen, V.; Monsalvo, V.M.; Sebastian, V. Advances in draw solutes for forward osmosis: Hybrid organic-inorganic nanoparticles and conventional solutes. *Chem. Eng. J.* **2017**, *309*, 738–752. [CrossRef]
54. Bui, N.-N.; Arena, J.T.; McCutcheon, J.R. Proper accounting of mass transfer resistances in forward osmosis: Improving the accuracy of model predictions of structural parameter. *J. Membr. Sci.* **2015**, *492*, 289–302. [CrossRef]
55. Touati, K.; Tadeo, F. Study of the reverse salt diffusion in pressure retarded osmosis: Influence on concentration polarization and effect of the operating conditions. *Desalination* **2016**, *389*, 171–186. [CrossRef]
56. Giagnorio, M.; Ricceri, F.; Tagliabue, M.; Zaninetta, L.; Tiraferri, A. Hybrid forward osmosis–nanofiltration for wastewater reuse: System design. *Membranes* **2009**, *9*, 61. [CrossRef]
57. Tran, T.T.D.; Park, K.; Smith, A.D. Performance analysis for pressure retarded osmosis: Experimentation with high pressure difference and varying flow rate, considering exposed membrane area. In Proceedings of the ASME 2016 International Mechanical Engineering Congress and Exposition IMECE2016, Phoenix, AZ, USA, 11–17 November 2016.
58. Zou, S.; Gu, Y.; Xiao, D.; Tang, C.Y. The role of physical and chemical parameters on forward osmosis membrane fouling during algae separation. *J. Membr. Sci.* **2011**, *366*, 356–362. [CrossRef]
59. Devia, Y.P.; Imai, T.; Higuchi, T.; Kanno, A.; Yamamoto, K.; Sekine, M. Effect of operating conditions on forward osmosis for nutrient rejection using magnesium chloride as a draw solution. *Int. J. Environ. Ecol. Eng.* **2015**, *9*, 691–696.
60. Akther, N.; Daer, S.; Hasan, S.W. Effect of flow rate, draw solution concentration and temperature on the performance of TFC FO membrane, and the potential use of RO reject brine as a draw solution in FO-RO hybrid systems. *Desalination Water Treat.* **2018**, *136*, 65–71. [CrossRef]
61. Deshmukh, A.; Yip, N.Y.; Lin, S.; Elimelech, M. Desalination by forward osmosis: Identifying performance limiting parameters through module-scale modeling. *J. Membr. Sci.* **2015**, *491*, 159–167. [CrossRef]

62. Cath, T.Y.; Elimelech, M.; McCutcheon, J.R.; McGinnis, R.L.; Achilli, A.; Anastasio, D.; Brady, A.R.; Childress, A.E.; Farr, I.V.; Hancock, N.T.; et al. Standard methodology for evaluating membrane performance in osmotically driven membrane processes. *Desalination* **2013**, *312*, 31–38. [CrossRef]
63. Zhao, S.; Zou, L.; Tang, C.Y.; Mulcahy, D. Recent developments in forward osmosis: Opportunities and challenges. *J. Membr. Sci.* **2012**, *396*, 1–21. [CrossRef]